

Thermal-fluid characterization of alternative liquids of power transformers: a numerical approach

Ramón Lecuna, Fernando Delgado, Alfredo Ortiz, Pablo B. Castro, Inmaculada Fernandez and Carlos J. Renedo

Mining and Energy Engineering School, Cantabria University
Bulevar Ronda Rufino Peón, s/n, 39316, Torrelavega, (Spain)
Phone/Fax number:+34 9422013 76/85; e-mail: ramon.lecuna@unican.es

ABSTRACT

The transformers lifespan depends importantly on its refrigeration. Mineral oils perform this work in the majority of the power transformers. However, this type of coolant has two main drawbacks: low biodegradability and low ignition point. Several alternative liquids are being developed in order to overcome these drawbacks. This paper compares their thermal-fluid behavior with a mineral oil by means of several parameters, such as temperature, flow rate, fluids velocity, convective heat transfer coefficient (h) and the cooling criterion (P). These are calculated using the numerical results of the simulation of a 3D-model of a Low Voltage Winding that belongs to a power transformer with ONAN cooling. The software COMSOL Multiphysics has allowed the simulation of the geometry using a physical model in which buoyancies and viscous forces are the only considered establishing the natural convection. As a result of the comparison, it is clear that the mineral oil is the best coolant liquid. Among the alternative liquids, silicone oil would be the second best coolant fluid, followed by the synthetic and natural esters, respectively. On the other hand, it seems to be clear that the 3D simulations can be used to compare properly the cooling capacities of the liquids.

Index Terms —Dielectric liquids, fluid-dynamics, thermal analysis, power transformers, numerical analysis

1. INTRODUCTION

1 MINERAL oil is the most common option as a cooling
2 and dielectric liquid in the majority of the power transformers
3 worldwide. However, in cases where fire risk is an important
4 concern, this type of liquid is not so recommendable. Fire
5 resistant oils (with higher flash and fire points than those of the
6 mineral oils) should be used. Environmental reasons are also
7 supporting the development of new transformer oils with
8 improved biodegradability, so that in the event of a failure or
9 leakage the impact would be lower. Thus, the growing
10 demands for improved fire safety and environmental
11 sustainability have encouraged the research and development
12 of alternative fluids.

14 The main research lines of these liquids are focused in
15 silicone oils, natural and synthetic esters. The characterization
16 of silicone oils and synthetic esters has been studied by a few
17 authors [1-5]. However, the majority of the studies has been
18 focused in the physicochemical characterization of some
19 commercial natural esters, [6-8], or based on some specific
20 crop (coconut, palm, rapeseed...) [9-10]. Finally, some authors
21 have compared the main properties of these new fluids with
22 mineral oil in order to evaluate their suitability [11].

23 On the other hand, there has been a lot of research about
24 cooling improvement in power transformers. The reason is
25 simple, high temperatures degrade the dielectric materials, oil
26 and paper, shortening their lifespan. In order to ensure a long
27 life for these machines, there are two types of approximations
28 for the calculation of their temperature and velocity
29 distributions: lumped parameter models and Computational
30 Finite Element-based Tools (CFET). The first method provides
31 fast and approximate results based on several simplifications
32 and empirical data. By contrast, the second one is more
33 accurate since it is based on the solution of the differential
34 equations governing processes.

35 Several papers have been published in last decade using CFET.
36 Nonetheless, we have to mention that the main goal of
37 practically all these papers is the determination of the velocity
38 and temperature profiles of a mineral oil inside a 2D section of
39 one winding. For instance, Mufuta and Van den Buck
40 described the flow pattern and its influence in the cooling of
41 the windings of a disc-type transformer by means of
42 dimensionless parameters (Nu , Re , Gr) applied on a 2D model
43 [12]. Six years later, El Wakil et al. studied the heat transfer
44 and fluid flow in two windings wound around a core of a step-
45 down 3-phase layer-type power transformer by means of the
46 analysis of six different 2D-models [13]. In 2007, Rahimpur et

47 al. calculated the influence of some parameters (heat loss,
 48 number of washers, height of the radiators and channel
 49 geometry) over temperatures distribution of a 2D-model of a
 50 natural convective cooled disc-type winding including block
 51 washers [14]. . Two years later, Smolka et al., in addition to
 52 perform a review about numerical simulations of the fluid
 53 flow, heat transfer and electromagnetic phenomena, presented
 54 an innovative 3D-coupled Computational Fluid Dynamics
 55 (CFD) and ElectroMAGnetic (EMAG) simulation of a 3-phase
 56 medium-power dry-type transformer [15]. In 2010, a 2D-
 57 model of a pass of a Low Voltage Winding (LVW) that
 58 belongs to a 3-phase disc-type transformer was simulated
 59 by Torriano et al. The main goal of this paper was to find
 60 the influence of different inlet conditions on the flow and
 61 temperature distributions. They also determined the location
 62 of the hot-spots in the winding [16]. More recently, in 2012,
 63 the same authors carried out a comparison between 2D and 3D
 64 models of the same geometry, thus determining the existence
 65 of three-dimensional fluid flow phenomena that cannot be
 66 obviated such as it occurs in the 2D-model [17]. The same
 67 year, Skillen et al. developed a 2D-model based on the
 68 geometry of Torriano's transformer with five passes in a
 69 column. The presence of hot-plumes in some horizontal ducts
 70 and the transmission of hot streaks from one pass to the next
 71 (flow coupling) were the main conclusions of this paper [18].
 72 Again, in the same year, a 3-D model of a 15-kVA ONAN
 73 transformer was carried out by Rosillo et al. in which oil
 74 velocity profile and oil and winding temperature distribution
 75 were calculated and experimentally validated in accordance
 76 with the IEEE-1995 Loading Guide [19]. Finally, one year
 77 before, Gastelurrutia et al. presented slices of several ONAN
 78 distribution transformers (2D-models) in which the oil flow
 79 and the thermal distributions were numerically calculated, thus
 80 allowing the comparison of the results with the experimental
 81 ones [20].

82 All the papers mentioned in former paragraph use mineral
 83 oil as dielectric liquid. Moreover, the majority of the models
 84 used were performed in two dimensions in order to overcome
 85 computational limitations. This type of 2D analysis is
 86 discarded in this paper due to there is heat transfer in all
 87 directions of the volume of our model; also, this 2D analysis
 88 does not allow determinate the exact location of the hot spots.
 89 For that reason, a 3D-section of the cooling ducts of the LVW
 90 of a real power transformer is used in this paper. Even more,
 91 this geometry is simulated using a physical model in which
 92 buoyancies and viscous forces are the only considered
 93 establishing the natural convection. As a result of this
 94 simulation, a comparison of the main characteristics of a
 95 mineral oil and three alternative liquids (a silicone oil, a natural
 96 ester and a synthetic ester) is obtained. In order to carry out this
 97 work, a thermal-fluid analysis has been performed using flow
 98 rates, temperature and velocity distributions and parameters
 99 such as the traditional convective heat transfer coefficient (h)
 100 and the new one cooling criterion (P).

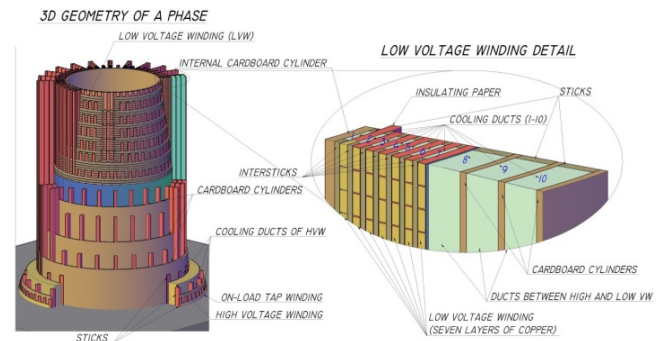
101 Section two presents a brief geometrical description of the
 102 3D model that is used. The third section introduces the
 103 numerical model considered. The studied parameters and the
 104 analysis methodology are presented in the fourth section.
 105 Simulation results and their comparison are shown in the fifth

106 section. Finally, findings are presented in the last section.

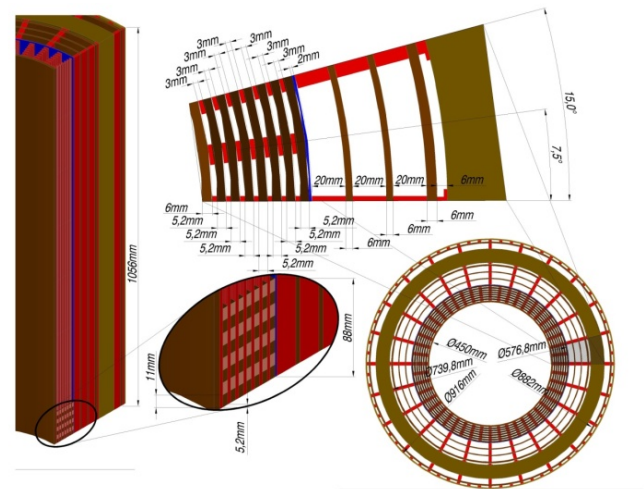
107 2. MODEL GEOMETRY DESCRIPTION

108 The aforementioned comparison has been carried out by
 109 using a section of the LVW of a three-phase power
 110 transformer. In nominal regime, the electrical
 111 characteristics of this transformer are 14 MVA, 66/6.3 kV,
 112 Dyn11 and ONAN cooling.

113 The self-explanatory Figure 1 (left side) and Figure 2
 114 (bottom right corner) shows the three windings of a phase
 115 of a three-phase transformer: LVW in the inner part;
 116 on-load tap winding in the outer part; finally, the High Voltage
 117 Winding in the middle of both of them.



119 **Figure 1.** 3D geometry of one phase and detail of the LVW



120 **Figure 2.** Plant dimensioning of a phase and detail of the LVW

121 The LVW, shown in 3D dimensions in the right side of
 122 Figure 1 and in 2D dimensions plan in the upper side of
 123 Figure 2, is composed of an internal cardboard cylinder (6
 124 mm thick and 450 mm of inner diameter) surrounded by 7
 125 concentric layers with 11 copper turns by layer. Each turn
 126 has 8 parallel plates (plate dimensions: 10.4mmx4.6mm)
 127 that are wrapped with a dielectric paper of 0.3 mm width.
 128 The layers are separated by means of 48 wooden sticks and
 129 inter-sticks of 3 mm thick. This way, 48 cooling ducts of
 130 7.5 degrees of amplitude are created between internal
 131 cylinder and first layer, other 48 cooling channels between
 132 first layer and second layer, and so on. Finally, the total
 133 height of the LVW is 1,056 mm.

134 Self-explanatory Figure 3 allows understanding how the
 135 geometrical design has evolved to achieve the optimal

136 model for solving numerically. In fact, the results
 137 comparison of both models (15-degree model and 7.5-
 138 degree model) allows to demonstrate that there are no
 139 significant differences between their temperatures and
 140 velocities distributions. This way, 7.5-degree model has
 141 been chosen.
 142

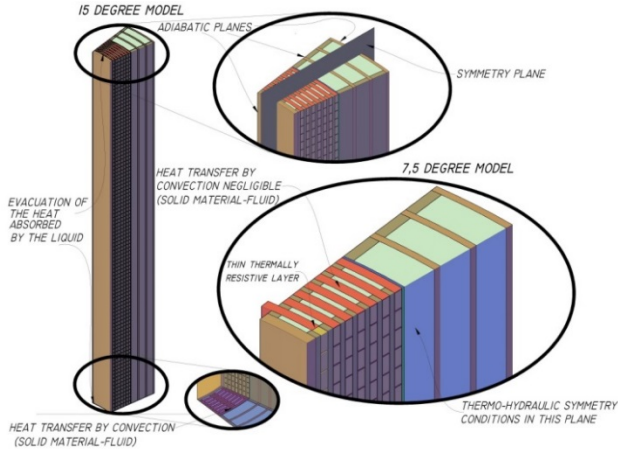


Figure 3. Geometrical evolution of the model

143 3. NUMERICAL MODEL

144 This section presents the governing equations, the
 145 physical model and its boundary conditions, computational
 146 domain and mesh.

147 3.1. GOVERNING EQUATIONS

148 This study is based on the numerical solution of the
 149 momentum and continuity equations, (1) and (2)
 150 respectively. It also solves the heat transfer equation, which
 151 for a fluid is (3).
 152

$$\rho(\mathbf{u} \cdot \nabla)\mathbf{u} = \nabla \cdot \left[-p\mathbf{I} + \mu(\nabla\mathbf{u} + (\nabla\mathbf{u})^T) - \frac{2}{3}\mu(\nabla \cdot \mathbf{u})\mathbf{I} \right] + \mathbf{F} \quad (1)$$

$$\nabla \cdot (\rho\mathbf{u}) = 0 \quad (2)$$

$$\rho C_p \mathbf{u} \cdot \nabla T = \nabla \cdot (k \nabla T) + q \quad (3)$$

153
 154 The symbols ρ , \mathbf{u} , p , \mathbf{I} , μ , \mathbf{F} , C_p , T and q of (1), (2) and
 155 (3) are density, velocity vector, pressure, identity matrix,
 156 dynamic viscosity, body force vector, specific heat
 157 capacity, temperature and unitary heat transfer,
 158 respectively.

159 3.2. PHYSICAL MODEL AND BOUNDARY 160 CONDITIONS

161 All exterior solid walls of the geometric model are
 162 considered adiabatic surfaces (see (4) in which k is the
 163 thermal conductivity) apart from the bottom solid surfaces.
 164 Also, the internal energy increase of the coolant between
 165 the oil inlets and outlets is considered (see details in left
 166 side of Figure 3).
 167

$$-\mathbf{n} \cdot (-k \nabla T) = 0 \quad (4)$$

168
 169 Convective cooling between the bottom solid surfaces
 170 and the oil is supposed, considering the inlet temperature of
 171 the liquid in the ducts as oil temperature ($T_{oil,inlet}=35^\circ\text{C}$) (see
 172 detail in bottom left side of Figure 3) (see (5) in which \mathbf{n} is
 173 the normal vector to boundary surface).

174

$$-\mathbf{n} \cdot (-k \nabla T) = h \cdot (T - T_{oil,inlet}) \quad (5)$$

175

176 No-slip condition is considered in the contact surfaces
 177 between oil and the solid surfaces in the ducts (see (6)).
 178

179

$$\mathbf{u} = 0 \quad (6)$$

180

181 Natural convection due to oil decreasing density with the
 182 increase of the temperature is the main phenomenon that
 183 determines the thermodynamic behavior inside the ducts
 184 (see (7) in which \mathbf{g} is the gravity acceleration). Also,
 185 boundary conditions in inlets and outlets of the cooling
 186 channels are pressure-based (see (8) for inlet pressure and
 187 (9) for outlet pressure in which $T_{oil,\infty}$, and H are the
 188 reference temperature of the model (35°C) and the total
 height of the ducts, respectively).

$$F_z = -g \cdot \rho(T); \rho(\mathbf{u} \cdot \nabla)\mathbf{u} = \nabla \cdot \left[-p\mathbf{I} + \mu(\nabla\mathbf{u} + (\nabla\mathbf{u})^T) - \frac{2}{3}\mu(\nabla \cdot \mathbf{u})\mathbf{I} \right] + \mathbf{F} \quad (7)$$

$$p = \rho(T_{oil,\infty}) \cdot g \cdot H; \left[\mu(\nabla\mathbf{u} + (\nabla\mathbf{u})^T) - \frac{2}{3}\mu(\nabla \cdot \mathbf{u})\mathbf{I} \right] \cdot \mathbf{n} = 0 \quad (8)$$

$$p = 0 \quad (9)$$

190

191 Thermal-fluid symmetry has been modeled using (10)
 192 and (11) (see detail in right-side of Figure 3).
 193

$$-\mathbf{n} \cdot (-k \nabla T) = 0 \quad (10)$$

$$\mathbf{u} \cdot \mathbf{n} = 0; \mathbf{K} - (\mathbf{K} \cdot \mathbf{n})\mathbf{n} = 0 \quad (11)$$

where

$$\mathbf{K} = [\mu(\nabla\mathbf{u} + (\nabla\mathbf{u})^T)]\mathbf{n}$$

194

195 The wrapping paper is considered mathematically as a
 196 thin thermally resistive layer whose thermal behavior is
 197 modeled according (12) in which k_p , T_i , T_o and d_p are the
 198 conductivity, the temperatures in the inside and outside
 199 surfaces and the thickness of the paper, respectively (see
 200 detail in right-side of Figure 3).
 201

$$q = -k_p \frac{(T_i - T_o)}{d_p} \quad (12)$$

202

203 Finally, a uniform volumetric heat source is considered
 204 in the copper domain using the Joule losses that are
 205 measured in a short-circuit test at 75°C of the power
 206 transformer (see (13) in which P_{Joule} and V are the copper
 207 loses in the 3-phase LVW and the volume of this winding,
 208 respectively).
 209

$$Q = \frac{P_{Joule}}{V} \quad (13)$$

210

211 The above physical model has been solved via the
 212 ‘‘Conjugate Heat Transfer’’ module of the commercial finite
 213 elements-based software Comsol Multiphysics v4.3a. This
 214 module allows combining the heat equation with either
 215 laminar or turbulent flow. The similarity between the
 216 geometric and physical models of our article and El-
 217 Morshedy’s paper [21], in addition to the higher viscosities
 218 of our coolants (water is the coolant of the reference
 219 article), allows us to establish that the heat transfer is going

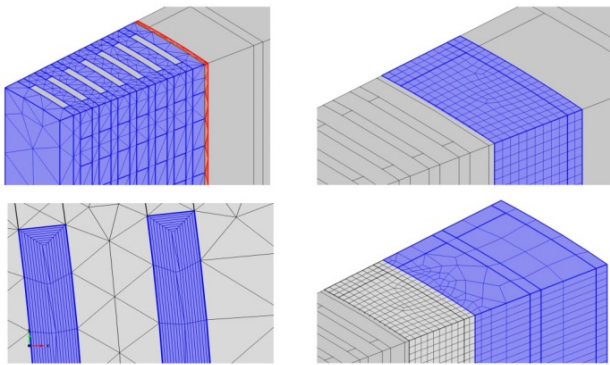
220 to be carried out by natural convection under laminar flow
221 regime.

222 3.3. COMPUTATIONAL DOMAIN AND MESH

223 The computational domain considers both the liquid and
224 solid parts of the geometry in order to calculate the
225 temperature distribution in the entire model and the fluid
226 behavior inside the channels. The simulations took between
227 90 and 120 minutes using a workstation with two
228 processors at 2.66 GHz and 48 Gbytes of RAM with a
229 convergence criterion of 10^{-4} for the residuals values.

230 Initially, in the meshing convergence study, several mesh
231 types with different meshing densities are studied, thus
232 obtaining several configurations with similar solutions. In
233 this paper, among these last configurations, the simplest one
234 from the computational standpoint is selected.

235 Three types of mesh and different element sizes were
236 used depending on the level of accuracy required.
237 Regarding the solid domain, it was meshed with a free
238 tetrahedral grid of 240,642 elements and a very thin
239 tetrahedral transitional mesh of 332,373 elements between
240 this domain and the first wide channel (See blue and red
241 volumes in upper left-side of Figure 4). 92,162 extra-thin
242 hexahedral elements were generated by means of a sweep
243 method applied between the bottom and upper faces of the
244 first channel (upper right-side of Figure 4). The other two
245 wide channels were meshed with the same method but with
246 a coarser element size, thus generating 127,574 elements
247 (bottom right-side of Figure 4). Finally, each of the seven
248 narrow channels was meshed by means of eight boundary
249 layers of 0.19 mm width, thus generating 264,570
250 tetrahedral elements (Bottom left-side of Figure 4).
251



252 **Figure 4.** Computational mesh of the solid and fluid domains

253 3.4. MATERIAL PROPERTIES

254 Figure 5 presents the four physical characteristics of the
255 five transformer liquids studied in this paper by means of
256 both their mathematical expressions and graphical plots in
257 the range of operating temperatures. These five dielectric
258 liquids are: one mineral oil, two silicone oils (one with
259 High Kinematic Viscosity (50 cSt, HKV) and other with
260 Low Kinematic Viscosity (25 cSt, LKV)), one natural ester
261 and one synthetic ester. The graphs are calculated using
262 data that are available in public datasheets since all of the
263 liquids are commercial oils.

264 The densities of these liquids decrease linearly with the
temperature. In the case of the viscosities, those of the

265 alternative liquids have higher values than mineral oil at
266 low temperatures, except the silicone oil with low viscosity.
267 However, this property diminishes exponentially with the
268 temperature, thus being practically equal at high
269 temperatures for all the liquids, except the silicon oil with
270 high viscosity.

271 The winding layers are made of copper conductors that
272 are individually wrapped with insulation paper. Also, these
273 layers and four cardboard cylinders are separated by
274 wooden sticks and inter-sticks. The physical properties (ρ ,
275 k , C_p) that are needed for all these materials in order to use
276 them in the simulations are shown in Table 1. These
277 properties are assumed to be constant with temperature.

278 Convective heat transfer coefficient at the bottom is
279 calculated considering a horizontal plate with down
280 external natural convection with oil at $T_{oil,inlet}=35^\circ\text{C}$.
281
282

Table1. Physical properties of solid materials

	ρ [kg/m ³]	k [W/(m K)]	C_p [J/(kg K)]
Copper	8,700	400	385
Paper	930	0.19	1,340
Cardboard	1,150	0.25	2,093.5
Wood	418.5	0.15	2,720

283

284

285 4. STUDY METHODOLOGY

286 The coefficient h can be used to determine the cooling
287 capacity of the fluids in order to carry out a thermal
288 comparison. This comparison can be performed using the
289 alternative parameter P . Equations (14) and (15) present the
290 way to calculate them by using the simulation results.

$$291 \quad h = \frac{Q_{ch}}{A \times (T_{avg,surface} - T_{oil,\infty})} \quad (14)$$

$$292 \quad P = \frac{C_p \times k \times \beta}{\nu} \quad (15)$$

$$293 \quad Q_{ch} = C_{p,avg} \times \dot{m}_{ch} \times (T_{avg,outlet} - T_{oil,inlet}) \quad (16)$$

294

295 The coefficient h is an experimentally determined
296 parameter which depends on many variables such as the
297 surface geometry, the nature of fluid motion and the
298 physical properties of the fluid. This coefficient allows
299 determining the efficiency of the heat transfer between a
300 solid surface and a fluid. The higher this number is, the
301 better the heat transfer by convection is. In this paper, it is
302 calculated according (14) in which Q_{ch} , A , $T_{avg,surface}$, are the
303 heat transfer between the copper and oil in each channel,
304 the heat transfer area of this channel and the average
305 temperature of this area, respectively. Q_{ch} is previously
306 estimated by means of the calculation of the internal energy
307 increase of the fluid between inlet and outlet surfaces (see
308 (16) in which the fluid properties $C_{p,avg}$, \dot{m}_{ch} , and $T_{avg,outlet}$
309 and $T_{oil,inlet}$ are considered). The average heat capacity, the
310 flow rate and the average temperature at the outlets of the
311 ducts are the meanings of the first three properties. Also,
the oil temperature in the ducts inlets ($T_{oil,inlet}$) is assumed as
reference temperature ($T_{oil,\infty}$).

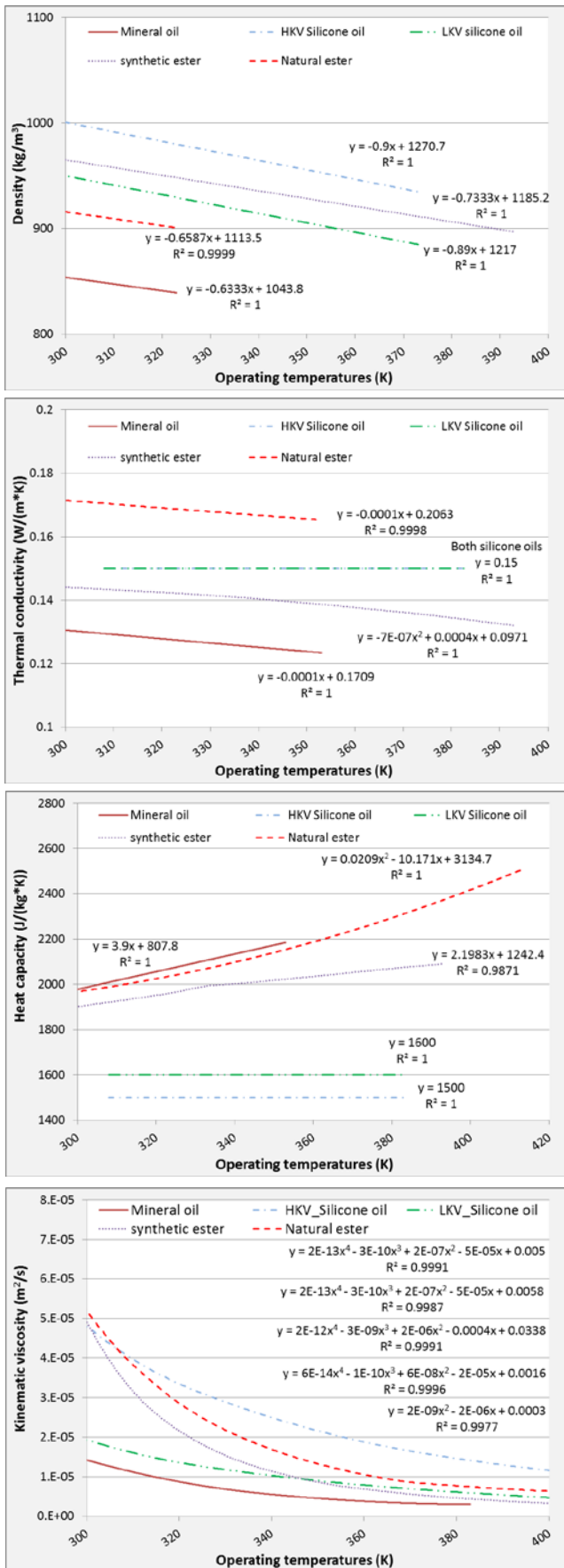


Figure 5. Physical properties of the dielectric liquids

313 The coefficient P depends on four physical properties of
 314 the fluids that vary with temperature (See (16) in which
 315 β and ν are the thermal expansion coefficient and the
 316 kinematic viscosity, respectively) and it is used in
 317 experimental studies to determine the heat transfer capacity
 318 of different oils [22]. Thus, the higher P is, the lower the
 319 average temperature of the fluid in each channel is. In each
 320 channel, it is calculated by means of (15) using the average
 321 values of the four properties.

322

5. RESULTS

323 The model validation is shown in the first subsection. In
 324 next subsection, temperatures and flow rates of the ducts
 325 are presented. Finally, in third subsection, a P results are
 326 compared.

327

5.1. MODEL VALIDATION

328 The comparison of the average velocities of the ducts 2-
 329 6, shown in Table 2, with those of the El-Morshedy's article
 330 [21] confirms the hypothesis that is initially supposed: the
 331 flow regime of all the studied liquids is laminar in those
 332 channels of our model that are similar, from the physical
 333 and geometric standpoint, to that of the aforementioned
 334 paper.
 335
 336

Table 2. Average velocities in the ducts ($V_{avg,duct}$)

	$V_{avg,duct}$ (mm/s)				
	Mineral oil	HKV Silicone oil	LKV Silicone oil	Synthetic ester	Natural ester
Channels 1	6.77	4.59	6.72	4.56	3.97
2	9.41	6.04	9.05	6.35	5.35
3	9.72	6.33	9.41	6.6	5.6
4	9.77	6.40	9.48	6.64	5.65
5	10.13	6.57	9.81	6.86	5.82
6	9.47	6.04	9.14	6.37	5.37
7	8.27	4.95	7.88	5.37	4.45
8	9.52	7.07	9.96	6.16	5.72
9	0.35	0.33	0.38	0.26	0.26
10	0.14	0.14	0.15	0.11	0.1

337

5.2. TEMPERATURES AND FLOW RATES

338 As initial point, it is necessary to point out that there are
 339 two types of channels from the geometrical standpoint:
 340 those ducts with narrow cross-section (channels 1-7), and
 341 those with wide cross-section (channels 8-10). It is clear
 342 that this geometrical feature has a major influence in the
 343 flow rates and velocities of the channels, therefore, in their
 344 temperatures (See Tables 2 and 3). Also, we can see that the
 345 velocities of those fluids with higher viscosities in the
 346 operating temperature range (ester-based liquid and HKV
 347 silicone oil) are lower than those of the other two liquids,
 348 both in narrow and wide channels.

349 Table 3 shows the maximum temperature of the
 350 geometry ($T_{max,model}$), the $T_{avg,outlet}$ and the \dot{m}_{ch} in all the
 351 ducts for all the liquids. In relation to the former, it can be

352 seen that if the alternatives liquids are used instead of the
 353 mineral oil there is an increase in the maximum
 354 temperatures. The location of these maximum temperatures
 355 (hot-spots) for all the oils can be seen in Figure 6. All of
 356 them are situated on the top of the geometry, in the middle
 357 of contact area of fourth stick with the third winding layer.
 358 This coincidence is justified in the fact that the location of
 359 the hot-spots depend only on the physical model developed,
 360 on the boundary conditions established and on the type of
 361 geometry considered. In other words, the location of the
 362 hot-spots doesn't depend on the type of liquid used in the
 363 coolant.
 364
 365

Table 3. Temperatures in the geometry and flow rates in cooling ducts

Channels	Mineral oil		HKV Silicone oil		LKV Silicone oil	
	$T_{avg,outlet}$ (°C)	\dot{m}_{ch} (g/s)	$T_{avg,outlet}$ (°C)	\dot{m}_{ch} (g/s)	$T_{avg,outlet}$ (°C)	\dot{m}_{ch} (g/s)
1	63.4	0.32	87.0	0.25	68.7	0.35
2	67.1	0.47	91.4	0.35	72.7	0.50
3	67.8	0.51	92.6	0.39	73.6	0.55
4	67.7	0.54	92.5	0.41	73.6	0.58
5	67.9	0.59	91.6	0.44	73.5	0.63
6	65.7	0.57	86.7	0.43	70.6	0.61
7	60.0	0.52	75.3	0.37	63.4	0.55
8	37.2	5.37	38.6	4.67	37.0	6.24
9	34.9	0.22	35.1	0.24	35.0	0.26
10	34.9	0.09	35.0	0.11	34.9	0.12
$T_{max,model}$ (°C)	71.8		96.3 ($\Delta T=24.5$)		77.5 ($\Delta T=5.7$)	

Channels	Synthetic ester		Natural ester	
	$T_{avg,outlet}$ (°C)	\dot{m}_{ch} (g/s)	$T_{avg,outlet}$ (°C)	\dot{m}_{ch} (g/s)
1	75.1	0.24	82.5	0.20
2	78.9	0.36	86.4	0.28
3	79.8	0.39	87.4	0.31
4	79.7	0.41	87.4	0.33
5	79.6	0.45	86.7	0.36
6	76.3	0.44	82.6	0.35
7	68.2	0.38	73.1	0.3
8	38.7	3.93	39.4	3.46
9	35.0	0.18	35.1	0.17
10	34.9	0.08	35.0	0.08
$T_{max,model}$ (°C)	82.9 ($\Delta T=11.1$)		89.9 ($\Delta T=18.1$)	

366

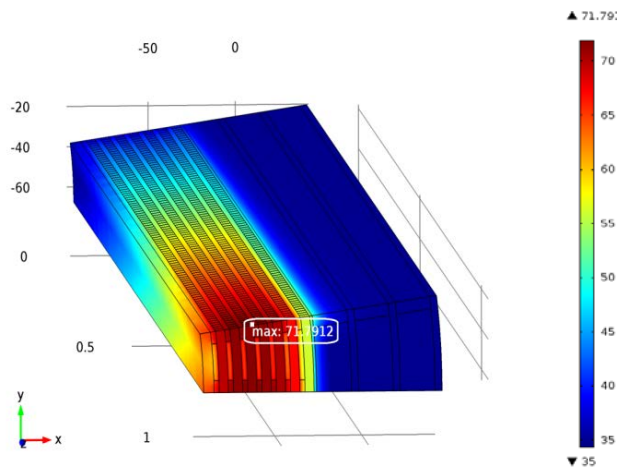


Figure 6. Location of hot-spots

367 From here, those channels with similar thermal behavior
 368 are going to be studied: the channels 2-5 have similar
 369 average temperatures inside them ($T_{avg,ch}$) and similar
 370 $T_{avg,outlet}$ for the same fluid (See Table 3 and Figure 7). Also,
 371 these channels have the highest temperatures if the same
 372 liquid is considered.

373 Then, it is perceived that the use of alternative fluids
 374 gives rise to an increase both in $T_{avg,outlet}$ and $T_{avg,ch}$. In both
 375 temperatures, the HKV silicone oil has the higher increment
 376 (36.1% and 25.4% respectively). On the other hand, the
 377 lower increment is in the case of LKV silicone oil (8.5%
 378 and 6.6% respectively). The ester-based oils have
 379 intermediate increments to those of the above. It is also
 380 remarkable that the higher is the $T_{avg,outlet}$, the smaller is
 381 $T_{avg,outlet}-T_{avg,ch}$. That is, higher temperature distributions in
 382 the ducts are obtained with the new liquids.
 383

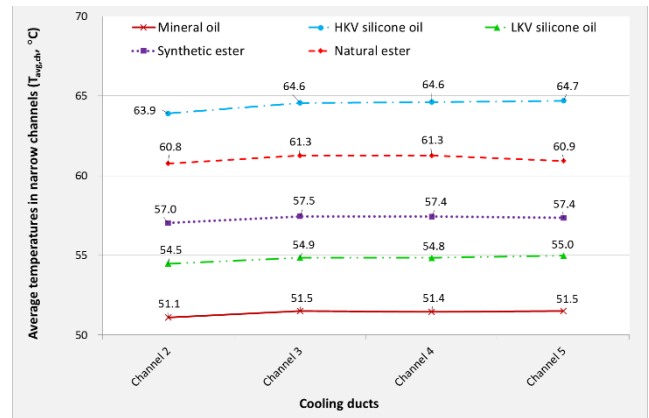


Figure 7. Average temperatures in narrow channels

384

385 Regarding the flow rates, shown in Table 3, it can be
 386 observed that mineral and LKV silicone oils have similar
 387 flow rates. In the range of operating temperatures, they both
 388 have similar viscosities. However, the mineral oil has
 389 higher specific heat capacity (and its value increases with
 390 the temperature) than that of the LKV silicone oil (its value
 391 is constant with the temperature). This fact explains why
 392 mineral oil is heated less than the LKV silicone-based fluid.
 393 As a result, the density variation of the mineral oil is
 394 smaller than that of the alternative liquid, thus obtaining a
 395 slightly lower flow rate. On the other hand, the ester-based
 396 liquids and HKV silicone oil have lower flow rates due to,
 397 mainly, their high viscosities in the aforementioned
 398 temperature range. In the case of ester-based fluids, the
 399 density decrease and specific heat capacity increase with
 400 the temperature does not completely offset the high viscous
 401 stresses. This effect is even more important in the case of
 402 the LKV silicone oil since the heat capacity is constant in
 403 the range of the operating temperatures. So, the cooling
 404 capacities of these last three alternative liquids are worse
 405 than those of the mineral and LKV silicone oils: there are
 406 higher temperatures in the winding, as can be seen in Table
 407 3 and Figure 7.

408

5.3. COOLING CAPACITY OF THE FLUIDS

409 Figure 8 shows the average values of the coefficients h of
 410 the five studied liquids in the channels two to five. As can
 411 be seen in this Figure, the higher coefficient h belongs to

412 mineral oil, with values in the range of 30 to 40 W/(m² K).
 413 The other coefficients are lower in a 13% (LKV silicone
 414 oil), 22% (synthetic ester), 32% (natural ester) and 40%
 415 (HKV silicone oil), approximately.

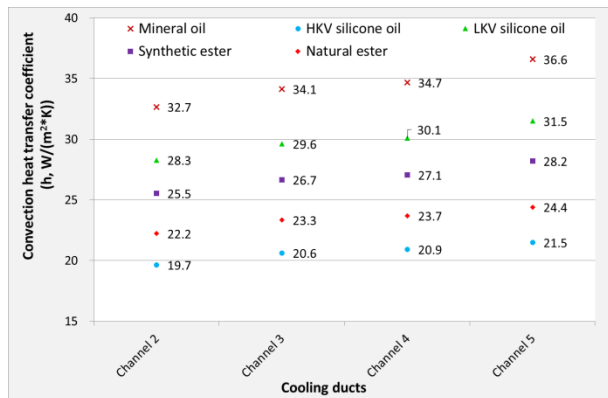


Figure 8. Average convection heat transfer coefficient of the liquids

417 In the same way that in the Figure 8, the average values
 418 of the P of the five studied liquids in the channels two to
 419 five are shown in Figure 9. Again, according to this parameter,
 420 mineral oil is the best coolant, followed by the LKV
 421 silicone oil, synthetic and natural esters, and HKV silicone
 422 oil (27%, 43%, 48% and 68% smaller values than mineral
 423 oil, respectively).

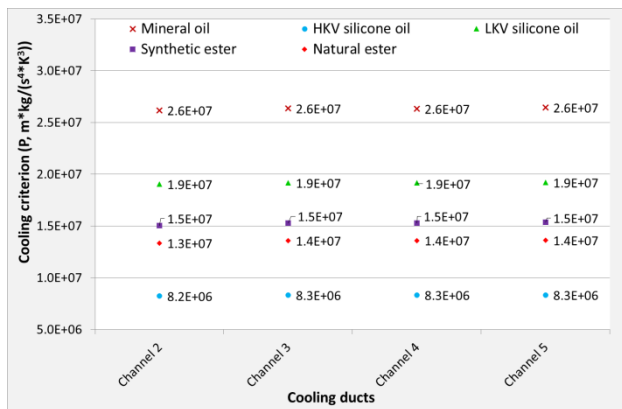


Figure 9. Average cooling criterion (P) of the liquids

426 There is an important difference between both
 427 parameters: P only considers the physical properties of the
 428 fluids and h also considers the flow characteristics in each
 429 channel. This fact explains why the values of h vary with
 430 the channel. However, the P values do not practically
 431 change with the channel. This also explains the higher
 432 differences in the cooling capacities between alternative
 433 liquids and the mineral oil using P instead of h .
 434 Nonetheless, it seems to be clear that the new parameter can
 435 also be used to classify the fluids according to their
 436 refrigeration capacities.

6. CONCLUSIONS

440 In the present study, the thermal-fluid behavior of five
 441 dielectric liquids (four alternative fluids and a traditional
 442 one) have been studied. In addition to the flow rates,

443 velocities and temperatures patterns are analyzed in order to
 444 establish thermal-fluid differences. Also, h and P are used
 445 to compare their cooling capacities. All the above is
 446 calculated using the numerical results of a 3D-model of a
 447 LVW of a transformer with ONAN cooling. This type of
 448 cooling has been performed by means of a physical model
 449 in which buoyancies and viscous forces are only
 450 considered.

451 As a result of the analysis of the aforementioned
 452 parameters, among the studied liquids, it is clear that the
 453 mineral oil is the better coolant, followed by the LKV
 454 silicone oil, synthetic ester, natural ester, and HKV silicone
 455 oil. It is remarkable that the viscosities of the biodegradable
 456 liquids and the HKV silicone oil are so high (especially with
 457 low temperatures) that their cooling capacities are
 458 negatively affected in an important manner, especially in
 459 the case of the HKV silicone oil. Regarding the LKV
 460 silicone oil, in comparison with the mineral oil, its main
 461 drawback is its worse specific heat capacity.

462 It seems to be clear that the 3D simulations can be used
 463 to compare properly the cooling capacities of the liquids
 464 using traditional parameters such as the convection heat
 465 transfer coefficient or new ones, such as the cooling
 466 criterion.

ACKNOWLEDGMENT

467 The research leading to these results has received
 468 funding from multiple sources during years but we would
 469 specifically like to acknowledge the support received in the
 470 later stages from the Spanish Plan Estatal de I+D under the
 471 grant agreement DPI2013-43897-P.

REFERENCES

- 473
 474 [1] E. Gockenbach, H. Borsi, Natural and synthetic ester liquids as
 475 alternative to mineral oil for power transformers. Presented at Annual
 476 Report Conference on Electrical Insulation and Dielectric Phenomena,
 477 CEIDP 2008, Quebec City, QC, 2008, pp. 521-524.
 478 [2] H. Borsi, E. Gockenbach, Properties of ester liquid midel 7131 as an
 479 alternative liquid to mineral oil for transformers. Presented at IEEE
 480 International Conference on Dielectric Liquids, ICDL 2005, Coimbra,
 481 2005, pp. 377-380.
 482 [3] R. Eberhardt, H. M. Muhr, W. Lick, B. Wieser, R. Schwarz, G. Pukel,
 483 Partial discharge behaviour of an alternative insulating liquid compared to
 484 mineral oil. Presented at IEEE International Symposium on Electrical
 485 Insulation, ISEI 2010, San Diego, CA, 2010.
 486 [4] H. Borsi, "Dielectric behavior of silicone and ester fluids for use in
 487 distribution transformers," *IEEE Trans Electr Insul*, vol. 26, pp. 755-762,
 488 10 September 1990 through 14 September 1990, 1991.
 489 [5] H. Kuwahara, K. Tsuruta, H. Munemura, T. Ishi, H. Shiomi, "Partial
 490 discharge characteristics of silicone liquids," *IEEE Trans Electr Insul*, vol.
 491 EI-11, pp. 86-91, 1976.
 492 [6] T. V. Oommen, C. C. Claiborne, E. J. Walsh, J. P. Baker, New
 493 vegetable oil based transformer fluid: Development and verification.
 494 Presented at IEEE Conference on Electrical Insulation and Dielectric
 495 Phenomena, BC, Can, 2000, pp. 308-312.
 496 [7] C. C. Claiborne, T. V. Oommen, E. J. Walsh, "Specification issues
 497 associated with the development of an agriculturally based biodegradable
 498 dielectric fluid," *ASTM Spec. Tech. Publ.*, pp. 37-46, 15 March 1999
 499 through 15 March 1999, 2000.
 500 [8] P. Boss, T. V. Oommen, New insulating fluids for transformers based
 501 on biodegradable high oleic vegetable oil and ester fluid. Presented at IEE
 502 Colloq. Dig., pp. 39-48, 1999.
 503 [9] U. U. Abdullahi, S. M. Bashi, R. Yunus, Mohibullah, H. A. Nurdin,
 504 The potentials of palm oil as a dielectric fluid. Presented at National Power
 505 and Energy Conference, PECon 2004, Kuala Lumpur, 2004, pp. 224-228.

506 [10] J. Li, S. Grzybowski, Y. Sun, X. Chen, Dielectric properties of
 507 rapeseed oil paper insulation, 2007 Annual Report - Conference on
 508 Electrical Insulation and Dielectric Phenomena, CEIDP, Vancouver, BC,
 509 2007, pp. 500-503.
 510 [11] I. Fernández, A. Ortiz, F. Delgado, C. Renedo, S. Pérez,
 511 "Comparative evaluation of alternative fluids for power transformers,"
 512 *Electr. Power Syst. Res.*, vol. 98, pp. 58-69, 2013.
 513 [12] J. -. Mufuta, E. Van Den Bulck, "Modelling of the mixed convection
 514 in the windings of a disc-type power transformer," *Appl. Therm. Eng.*, vol.
 515 20, pp. 417-437, 2000.
 516 [13] N. El Wakil, N. -. Chereches, J. Padet, "Numerical study of heat
 517 transfer and fluid flow in a power transformer," *Int. J. Therm. Sci.*, vol. 45,
 518 pp. 615-626, 2006.
 519 [14] E. Rahimpour, M. Barati and M. Schäfer, "An investigation of
 520 parameters affecting the temperature rise in windings with zigzag cooling
 521 flow path," *Appl. Therm. Eng.*, vol. 27, pp. 1923-1930, 2007.
 522 [15] J. Smolka, O. Bíró, A. J. Nowak, "Numerical simulation and
 523 experimental validation of coupled flow, heat transfer and electromagnetic
 524 problems in electrical transformers," *Arch. Comput. Methods Eng.*, vol. 16,
 525 pp. 319-355, 2009.
 526 [16] F. Torriano, M. Chaaban, P. Picher, "Numerical study of parameters
 527 affecting the temperature distribution in a disc-type transformer winding,"
 528 *Appl. Therm. Eng.*, vol. 30, pp. 2034-2044, 2010.
 529 [17] F. Torriano, P. Picher, M. Chaaban, "Numerical investigation of 3D
 530 flow and thermal effects in a disc-type transformer winding," *Appl. Therm.*
 531 *Eng.*, vol. 40, pp. 121-131, 2012.
 532 [18] A. Skillen, A. Revell, H. Iacovides, W. Wu, "Numerical prediction of
 533 local hot-spot phenomena in transformer windings," *Appl. Therm.*
 534 *Eng.*, vol. 36, pp. 96-105, 2012.
 535 [19] M. E. Rosillo, C. A. Herrera and G. Jaramillo, "Advanced thermal
 536 modeling and experimental performance of oil distribution transformers,"
 537 *IEEE Trans Power Delivery*, vol. 27, pp. 1710-1717, 2012.
 538 [20] J. Gastelurrutia, J. C. Ramos, G. S. Larraona, A. Rivas, J. Izagirre, L.
 539 Del Río, "Numerical modelling of natural convection of oil inside
 540 distribution transformers," *Appl. Therm. Eng.*, vol. 31, pp. 493-505, 2011.
 541 [21] S. E. D. El-Morshedy, A. Alyan, L. Shouman, "Experimental
 542 investigation of natural convection heat transfer in narrow vertical
 543 rectangular channel heated from both sides," *Exp. Therm. Fluid Sci.*, vol.
 544 36, pp. 72-77, 2012.
 545 [22] C. Perrier, A. Beroual, J. -. Bessede, "Improvement of power
 546 transformers by using mixtures of mineral oil with synthetic esters," *IEEE*
 547 *Trans. Dielectr. Electr. Insul.*, vol. 13, pp. 556-564, 2006.



Ramón Lecunawas was born in Torrelavega, on July 14, 1967. He received the M.Sc. degree in industrial engineering in 2000 and he is currently pursuing the Ph.D. degree from the University of Cantabria (UC), Spain. Currently, he is Assistant Professor in the Electrical and Energy Engineering Department of the UC. He has published 1 work in international conferences. Finally, his main research topic is currently the study of the alternative dielectric liquids in power transformers.

549



Fernando Delgado was born in Santander, on March 26, 1968. He received the M.Sc. degree in industrial engineering in 1998 and the Ph.D. degree in 2011 from the University of Cantabria (UC), Spain. Currently, he is Associate Professor in the Electrical and Energy Engineering Department of the UC. He has published over 25 works in international conferences and 13 papers in journals included in the Journal of Citation Report. Finally, his main research topic is currently the

550

study of the alternative dielectric liquids in power transformers.



Alfredo Ortiz was born in Santander, on September 9, 1971. He received the M.Sc. degree in industrial engineering in 1997 and the Ph.D. degree in 2005 from the University of Cantabria (UC), Spain. Currently, he is Associate Professor and the Head of Electrical and Energy Engineering Department at the UC. He has published six chapters in international books, over 50 works in international conferences and XX papers in journals included in the Journal of Citation Report. Finally, his main research topic is currently the study of the alternative dielectric liquids in power transformers.

551



Pablo B. Castrowas was born in Gijón, on July 12, 1979. He received the M.Sc. degree in industrial engineering in 2004 and the Ph.D. degree in 2011 from the University of Valladolid (UVA), Spain. Currently, he is Assistant Professor of Electrical and Energy Engineering Department at the UC. He has published 10 works in international conferences and 7 papers in journals included in the Journal of Citation Report. Finally, his main research topic is currently computational fluid dynamics and numerical heat transfer, renewable energies and energy efficiency.

552



Inmaculada Fernández was born in Zaragoza, on July 31, 1981. He received the M.Sc. degree in chemical engineering in 2004 and the Ph.D. degree in 2009 from the University of Cantabria (UC), Spain. Currently, he is Assistant Professor in the Electrical and Energy Engineering Department of the UC. He has published two chapters in international books, over 20 works in national and international conferences and 9 papers in journals included in the Journal of Citation Report. Finally, his main research topic is the energy saving.

553



Carlos J. Renedowas was born in Santander, on November 03, 1969. He received the M.Sc. degree in industrial engineering in 1997 and the Ph.D. degree in 2002 from the University of Cantabria (UC), Spain. Currently, he is Associate Professor in the Electrical and Energy Engineering Department of the UC and Vicedean of the School of Industrial Engineering and Telecommunications. He has published over 50 works in international conferences and 24 papers in journals included in the Journal of Citation Report. Finally, his main research topic is the energy saving.

554